Bioorganic Chemistry 107 (2021) 104530

Contents lists available at ScienceDirect

Bioorganic Chemistry

journal homepage: www.elsevier.com/locate/bioorg

Bioactive sesquiterpene derivatives from mangrove endophytic fungus *Phomopsis* sp. SYSU-QYP-23: Structures and nitric oxide inhibitory activities

Yan Chen [a,b], Hongju Liu [c], Ge Zou [a], Wencong Yang [a], Lishan Zhang [c], Zhangyuan Yan [d], Yuhua Long [d,*], Zhigang She [a,*]

[a] School of Chemistry, Sun Yat-Sen University, Guangzhou 510275, PR China
[b] National R & D Center for Edible Fungus Processing Technology, Henan University, Kaifeng 475004, China
[c] School of Pharmacy, Guangdong Medical University, Dongguan 523808, PR China
[d] School of Chemistry, South China Normal University, Guangzhou 510006, PR China

ARTICLE INFO

Keywords:
Phomopsis sp.
Mangrove endophytic fungus
Sesquiterpene derivatives
Anti-inflammatory activity
Molecular docking

ABSTRACT

Eight new sesquiterpene derivatives (**2**, **4**–**6** and **10**–**13**), along with five known analogues were isolated from the mangrove endophytic fungus *Phomopsis* sp. SYSU-QYP-23. Their structures of new compounds were established by spectroscopic methods, and the absolute configurations were confirmed by single-crystal X-ray diffraction analysis and comparison of the experimental ECD spectra. The absolute configuration of the side chain in **1** was first defined by modified Mosher's method. Compounds **1**–**7** showed potent inhibitory activities against nitric oxide (NO) production in lipopolysaccharides (LPS) induced RAW 264.7 cells with IC_{50} values ranging from 8.6 to 14.5 μM. The molecular docking results implied that the bioactive sesquiterpenes may directly bind with targeting residues in the active cavity of iNOS protein.

1. Introduction

Sesquiterpenes, the largest members in the terpenoid family, were produced from diverse genera of higher plants, insects, terrestrial fungi, and various marine organisms [1,2], and possessed a wide range of pharmacological activities including cytotoxic, anti-inflammatory, antimalarial, antibacterial, antifungal, anti-hyperlipidemic, and anti-viral [3–7]. The fungal genus *Phomopsis* was commonly isolated from terrestrial or marine-derived environments and produced various biologically active secondary metabolites [8,9], for example, sesquiterpene phomoarcherin B with antimalarial activity [10], polyketone lithocarols A-E with cytotoxic activities [11] and alkaloid farinomaleins A-B with anti-inflammatory activities [12]. A previous chemical investigation of *Phomopsis* sp. SYSU-QYP-23 cultured in solid medium resulted in six new alkaloids [12], which showed strong inhibitory activities against nitric oxide (NO) production in lipopolysaccharides (LPS) induced RAW 264.7 cells. In a continuing searching for more natural anti-inflammatory products, the strain were further fermented in liquid medium, leading to the isolation of eight new ones (**2**, **4**–**6** and **10**–**13**) and five known analogues (**1**, **3** and **7**–**9**). The nitric oxide (NO) inhibitory activity of all isolates were tested. Herein, we report the isolation, structure elucidation, and biological functions of these isolated compounds, as well as the molecular docking study of bioactive compounds.

2. Experimental

2.1. General experimental procedures

Melting points were measured on a Fisher-Johns hot-stage apparatus. Optical rotations, IR spectra, 1D and 2D NMR experiments, and HRESIMS spectra were performed using the same instruments as previously published paper [12]. ECD data were recorded on a Chirascan CD spectrometer (Applied Photophysics).

2.2. Fungal material, fermentation, extraction and isolation

The strain *Phomopsis* sp. SYSU-QYP-23 was described as previously reported [12]. It was cultured on PDA medium for five days. Then, the seed culture was prepared by the mycelium of the fungus inoculating into 200 mL PDB medium for three days. Thereafter, the seed culture was transferred into liquid medium (potato 7 kg, dextrose 20 g/L, and artifical sea salts 20 g/L, 100 × 1000 flasks) at 28 °C for 30 days.

* Corresponding authors.
E-mail addresses: longyh@scnu.edu.cn (Y. Long), cesshzhg@mail.sysu.edu.cn (Z. She).

https://doi.org/10.1016/j.bioorg.2020.104530
Received 6 August 2020; Received in revised form 30 October 2020; Accepted 30 November 2020
Available online 3 December 2020
0045-2068/Published by Elsevier Inc.

Table 1
^{1}H NMR (500 MHz) spectroscopic data for compounds **2** and **4**–**6** in $CDCl_3$ (δ in ppm, J in Hz).

no.	2	4	5	6
1	2.49, dt (4.5, 15.0)	2.49, dt (3.4, 14.6)	2.49, m	2.32, m
	2.35, m	2.35, m	2.36, m	2.16, m
2	2.17, m	2.17, q (12.3)	2.18, q (11.5)	2.03, dt (3.4, 8.3)
	1.48, m	1.49, brd (13.9)	1.48, brd (10.2)	1.40, dd (4.4, 14.3)
3	4.89, dt (4.4, 11.6)	4.91, dt (4.4, 11.1)	4.91, dt (4.4, 11.1)	4.85, m
4	1.65, m	1.63, m	1.63, qd (6.7, 11.0)	1.54, m
6	2.04, dd (4.5, 13.1)	2.03, dd (4.5, 13.0)	2.03, dd (4.5, 13.0)	1.60, m
	1.89, t (13.1)	1.90, m	1.87, m	
7	3.13, dd (4.5, 14.4)	3.11, dd (4.5, 14.4)	3.11, dd (4.5, 14.4)	2.24, m
8				4.09, brs
9	5.78, brs	5.79, brs	5.79, brs	5.64, d (5.6)
12	5.01, brs	5.0, brs	5.0, brs	5.02, brs
	4.83, brs	4.82, brs	4.82, brs	4.82, brs
13	1.74, s	1.74, s	1.74, s	1.83, s
14	0.96, d (6.6)	0.96, d (6.7)	0.96, d (6.7)	0.92, d (6.7)
15	1.20, s	1.23, s	1.23, s	1.0, s
2′	2.67, quint (7.0)	2.58, quint (7.2)	2.58, quint (7.2)	2.58, quint (7.1)
3′	4.44, m	4.25, dt (5.0, 7.2)	4.24, dt (5.3, 7.2)	4.23, brt (7.1)
4′	5.62, dd (6.1, 15.2)	5.76, dd (5.0, 15.2)	5.81, dd (5.3, 15.2)	5.59, dd (6.8, 15.2)
5′	6.28, dd (10.3, 15.2)	5.76, dd (10.3, 15.2)	5.81, dd (10.3, 15.2)	6.26, dd (10.3, 15.2)
6′	6.12, dd (10.3, 15.0)	4.25, dd (10.3, 11.3)	4.20, m	6.12, dd (10.3, 15.1)
7′	5.73, td (7.4, 15.0)	4.14, td (6.3, 11.3)	4.14, td (2.8, 6.1)	5.71, td (7.4, 15.1)
8′	2.30, m	2.40, m	1.96, m	2.25, m
	2.24, m	1.61, m	1.71, m	
9′	3.86, qd (6.1, 11.8)	4.22, m	4.30, m	3.85, qd (6.2, 12.0)
10′	1.23, d (6.1)	1.33, d (6.2)	1.30, d (6.0)	1.20, d (6.2)
11′	1.22, d (7.2)	1.20, d (7.2)	1.20, d (7.2)	1.18, d (7.2)

Thereafter, the broth was extracted with EtOAc three times, and the mycelia was extracted with MeOH twice. Both of the organic phases were combined and evaporated under reduced pressure to yield the extracts of 30.5 g. Then, the residue was fractionated by silica gel column chromatography with a gradient of petroleum ether/EtOAc from 10:0 to 0:10 to give ten fractions (Fr.1- Fr.10). Fr.2 (2.3 g) was subjected to silica gel CC (CH_2Cl_2/MeOH v/v, 98:2) to yield compound **8** (3.6 mg). Fr.3 was subjected to silica gel CC (CH_2Cl_2/MeOH v/v, 97:3) to yield compound **9** (3.3 mg) and an additional Fr.3.1 which was purified by semipreparative reversed-phase HPLC (MeOH-H_2O, 75:25) to yield compounds **4** (2.6 mg) and **5** (3.0 mg). Fr.4 was subjected to silica gel CC (CH_2Cl_2/MeOH v/v, 88:12) to yield compound **7** (3.3 mg). Fr.5 (5 g) was purified by Sephadex LH-20 CC (CH_2Cl_2/MeOH v/v, 1:1) to afford two fractions (Fr.5.1 and 5.2). Fr.5.1 was subjected to silica gel CC (CH_2Cl_2/MeOH v/v, 91:9) to give compounds **1** (35.5 mg) and **6** (2.3 mg). Fr.5.2 was subjected to silica gel CC (CH_2Cl_2/MeOH v/v, 89:11) to yield compound **2** (3.7 mg) and an additional fraction Fr.5.2.1 which was purified by Sephadex LH-20 CC (CH_2Cl_2/MeOH v/v, 1:1) to give compound **10** (6.8 mg). Fr.6 (45.3 g) was purified by Sephadex LH-20 CC (CH_2Cl_2/MeOH v/v, 1:1) to obtain three fractions (Fr.6.1- Fr.6.3). Fr.6.1 was subjected to silica gel CC (CH_2Cl_2/MeOH v/v, 83:17) to yield compound **3** (5.0 mg). Fr.6.2 was subjected to silica gel CC (CH_2Cl_2/MeOH v/v, 82:18) to yield compound **11** (3.5 mg). Fr.7 was applied to silica gel CC (CH_2Cl_2/MeOH v/v, 82:18) to give compound **13** (4.0 mg) and an additional fraction Fr.7.1 which was purified by semipreparative reversed-phase HPLC (MeOH-H_2O, 70:30) to obtain compound **12** (3.5 mg).

Eremofortin G (**2**): colorless oil; $[\alpha]_D^{25}$ +18 (c 0.20, MeOH); UV (MeOH) λ_{max} (log ε): 235(3.50) nm; IR (KBr) ν_{max}: 3453, 2947, 1735, 1626, 1433, 1342, 1228 cm^{-1}; ^{1}H and ^{13}C NMR data, see Tables 1 and 2; HRESIMS m/z 431.27928 $[M + H]^+$ (calcd for $C_{26}H_{39}O_5$, 431.27920).

Eremofortin H (**4**): colorless oil; $[\alpha]_D^{25}$ +23 (c 0.22, MeOH); UV (MeOH) λ_{max} (log ε): 234(3.47) nm; IR (KBr) ν_{max}: 3426, 2952, 1726, 1656, 1450, 1368, 1260, 1172 cm^{-1}; ^{1}H and ^{13}C NMR data, see Tables 1 and 2; HRESIMS m/z 447.27375 $[M + H]^+$ (calcd for $C_{26}H_{39}O_6$, 447.27412).

Eremofortin I (**5**): colorless oil; $[\alpha]_D^{25}$ +18 (c 0.20, MeOH); UV (MeOH) λ_{max} (log ε): 235(3.50) nm; IR (KBr) ν_{max}: 3436, 2942, 1718, 1635, 1443, 1352, 1236 cm^{-1}; ^{1}H and ^{13}C NMR data, see Tables 1 and 2; HRESIMS m/z 447.27364 $[M + H]^+$ (calcd for $C_{26}H_{39}O_6$, 447.27412).

Eremofortin J (**6**): colorless oil; $[\alpha]_D^{25}$ +16 (c 0.25, MeOH); UV (MeOH) λ_{max} (log ε): 235(3.56) nm; IR (KBr) ν_{max}: 3432, 2967, 1716, 1662, 1462, 1375, 1258, 1176 cm^{-1}; ^{1}H and ^{13}C NMR data, see Tables 1 and 2; HRESIMS m/z 455.27709 $[M + Na]^+$ (calcd for $C_{26}H_{40}NaO_5$, 455.27680).

Altiloxin C (**10**): White hydrate crystals; $[\alpha]_D^{25}$ −27 (c 0.31, MeOH); UV (MeOH) λ_{max} (log ε): 220 (3.42) nm; IR (KBr) ν_{max}: 3468, 3414, 2931, 1728, 1700, 1382, 1276, 1246 cm^{-1}; ^{1}H and ^{13}C NMR data, see Tables 2 and 3; HRESIMS m/z 303.13731 $[M-H]^-$ (calcd for $C_{15}H_{24}ClO_4$, 303.13686).

Altiloxin D (**11**): White solid; $[\alpha]_D^{25}$ −65 (c 0.85, MeOH); UV (MeOH) λ_{max} (log ε): 220 (3.86) nm; IR (KBr) ν_{max}: 3445, 2962, 1735, 1675, 1363, 1256, 1218 cm^{-1}; ^{1}H and ^{13}C NMR data, see Tables 2 and 3; HRESIMS m/z 267.16018 $[M-H]^-$ (calcd for $C_{15}H_{23}O_4$, 267.16018).

Altiloxin E (**12**): White hydrate crystals; $[\alpha]_D^{25}$ −43 (c 0.52, MeOH); UV (MeOH) λ_{max} (log ε): 220 (3.55) nm; IR (KBr) ν_{max}: 3460, 3385, 2912, 1733, 1365, 1247 cm^{-1}; ^{1}H and ^{13}C NMR data, see Tables 2 and 3; HRESIMS m/z 275.1618 $[M + Na]^+$ (calcd for $C_{15}H_{24}NaO_3$, 275.1611).

Phomomane (**13**): White crystals; $[\alpha]_D^{25}$ −47 (c 0.48, MeOH); UV (MeOH) λ_{max} (log ε): 220 (3.65) nm; IR (KBr) ν_{max}: 3458, 2956, 1726, 1665, 1321, 1227 cm^{-1}; ^{1}H and ^{13}C NMR data, see Tables 2 and 3; HRESIMS m/z 253.18128 $[M-H]^-$ (calcd for $C_{15}H_{25}O_3$, 253.18092).

2.3. X-ray crystallographic analysis of compounds *10*, *12* and *13*

Single crystals of **10, 12** and **13** were obtained from MeOH solution. The data obtained on an Agilent Xcalibur Nova singlecrystal diffractometer using Cu kα radiation (λ = 1.5418 Å). The structures were solved by direct methods using SHELXS-97 software and refined with SHELXS-97 using by full-matrix least-squares, with anisotropic displacement parameters for all the non-hydrogen atoms. The crystallographic data can be obtained free of charge from the Cambridge Crystallographic Data Centre, 12 Union Road, Cambridge CB2 1EZ, UK (fax: 44-(0)1223-336033; e-mail: deposit@ccdc.cam.ac.uk).

Crystal data of **10**: $C_{15}H_{25}ClO_4{\cdot}H_2O$, M_r = 322.1, monoclinic, α = 7.6804(2) Å, b = 9.4260(3) Å, c = 10.9238(2) Å, α = 90.00°, β = 96.90°, γ = 90.00°, V = 788.09(4) Å^3, space group $P2_1$, Z = 2, T = 293(2) K, D_{calcd} = 1.360 g/cm^3, μ = 2.316 mm^{-1}, and F(000) = 348.0. Crystal dimension: 0.25 × 0.15 × 0.10 mm^3. Independent reflections: 3077 (R_{int} = 0.0395). The final R_1 values were 0.0634, wR_2 = 0.1566 (I> = 2σ (I)). The goodness of fit on F^2 was 1.080. Flack parameter = −0.03(2). CCDC number: 1977144.

Crystal data of **12**: $C_{15}H_{24}O_3$, M_r = 252.1, monoclinic, α = 6.3767(2) Å, b = 7.2885(2) Å, c = 16.8669(6) Å, α = 80.903°, β = 79.880(10)°, γ = 66.813°, V = 705.95(4) Å^3, space group $P1$, Z = 1, T = 150 K, D_{calcd} = 1.187 g/cm^3, μ = 0.645 mm^{-1}, and F(000) = 276.0. Crystal dimension: 0.30 × 0.15 × 0.02 mm^3. Independent reflections: 24,488 (R_{int} = 0.0560). The final R_1 values were 0.0945, wR_2 = 0.3005 (I> = 2σ (I)). The goddess of fit on F^2 was 1.129. Flack parameter = −0.04(16). CCDC number: 1977147.

Crystal data of **13**: $C_{15}H_{28}O_4$, M_r = 254.1, monoclinic, α = 6.1447(3)

Table 2
^{13}C NMR (125 MHz) spectroscopic data for compounds **2**, **4**–**6** and **10**–**13** (δ in ppm).

no.	2[a]	4[a]	5[a]	6[a]	10[b]	11[b]	12[b]	13[a]
1	30.6, CH_2	30.5, CH_2	30.5, CH_2	30.3, CH_2	34.3, CH_2	42.9, CH_2	40.4, CH_2	216.0, C
2	31.6, CH_2	31.5, CH_2	31.5, CH_2	32.4, CH_2	30.6, CH_2	42.6, CH_2	27.8, CH_2	34.8, CH_2
3	74.0, CH	73.8, CH	73.8, CH	74.9, CH	70.3, CH	19.4, CH_2	78.4, CH	37.1, CH_2
4	47.2, CH	47.0, CH	47.2, CH	47.5, CH	46.0, C	37.1, C	43.3, C	72.1, C
5	40.1, C	40.0, C	40.0, C	39.6, C	78.5, C	149.8, C	148.8, C	55.3, CH
6	41.7, CH_2	41.6, CH_2	41.6, CH_2	35.3, CH_2	27.0, CH_2	118.0, CH	119.7, CH	70.2, CH
7	50.3, CH	50.3, CH	50.3, CH	42.0, CH	38.3, CH_2	44.7, CH_2	44.5, CH_2	51.1, CH
8	195.3, C	198.5, C	198.7, C	63.6, CH	72.6, C	71.0, C	70.8, C	18.0, CH_2
9	124.8, CH	124.7, CH	124.7, CH	121.5, CH	59.2, CH	65.3, CH	65.2, CH	34.6, CH_2
10	166.0, C	166.4, C	166.3, C	147.1, C	42.6, C	40.7, C	40.3, C	46.9, C
11	143.3, C	143.2, C	143.3, C	146.3, C	176.7, C	176.4, C	176.2, C	25.5, CH
12	114.6, CH_2	114.4, CH_2	114.5, CH_2	112.1, CH_2	24.8, CH_3	25.0, CH_3	24.7, CH_3	21.1, CH_3
13	20.2, CH_3	20.0, CH_3	20.0, CH_3	22.9, CH_3	24.6, CH_3	21.5, CH_3	28.3, CH_3	15.9, CH_3
14	10.5, CH_3	10.5, CH_3	10.4, CH_3	10.9, CH_3	19.4, CH_3	33.6, CH_3	23.2, CH_3	18.8, CH_3
15	17.2, CH_3	17.2, CH_3	17.2, CH_3	18.1, CH_3	19.0, CH_3	29.8, CH_3	21.5, CH_3	25.9, CH_3
1′	175.2, C	175.0, C	175.0, C	175.4, C				
2′	45.2, CH	45.6, CH	45.6, CH	45.8, CH				
3′	72.7, CH	74.0, CH	73.8, CH	74.4, CH				
4′	130.7, CH	132.2, CH	131.8, CH	131.6, CH				
5′	131.8, CH	131.4, CH	131.7, CH	132.2, CH				
6′	132.5, CH	84.8, CH	86.5, CH	132.6, CH				
7′	131.0, CH	77.0, CH	77.4, CH	131.2, CH				
8′	42.5, CH_2	41.7, CH_2	42.1, CH_2	42.6, CH_2				
9′	67.3, CH	74.0, CH	74.5, CH	67.5, CH				
10′	22.9, CH_3	22.3, CH_3	21.0, CH_3	23.0, CH_3				
11′	11.6, CH_3	14.2, CH_3	14.1, CH_3	14.3, CH_3				

[a] Measured in $CDCl_3$.
[b] Measured in CD_3OD.

Å, b = 8.5787(4) Å, c = 14.1099(6) Å, α = 90.00°, β = 93.47°, γ = 90.00°, V = 742.42(6) Å^3, space group $P2_1$, Z = 2, T = 293(2) K, D_{calcd} = 1.218 g/cm^3, μ = 0.696 mm^{-1}, and F(0 0 0) = 300.0. Crystal dimension: 0.22 × 0.15 × 0.08 mm^3. Independent reflections: 2828 (R_{int} = 0.0346). The final R_1 values were 0.0579, wR_2 = 0.1581 (I>=2σ (I)). The goddess of fit on F^2 was 1.044. Flack parameter = − 0.14(18). CCDC number: 1977150.

Table 3
^{1}H NMR (500 MHz) spectroscopic data for compounds **10**–**13** (δ_H in ppm, J in Hz).

no.	10[a]	11[a]	12[a]	13[b]
1	1.95, m	1.76, m	1.65, dt (3.3, 13.3)	
	1.09, m	1.34, m	1.30, dt (3.6, 13.6)	
2	2.04, m	1.50, m	1.73, m	2.58, ddd (5.6, 10.5, 15.8)
	1.91, m	1.26, m	1.55, ddd (3.7, 7.7, 13.1)	2.41, ddd (4.6, 6.7, 15.8)
3	4.43, dd (4.7, 12.3)	1.87, m	3.05, dd (4.5, 11.7)	1.94, m
		1.49, m		
6	1.94, m	5.44, dd (3.2, 4.8)	5.44, dd (3.3, 4.8)	3.88, t (10.2)
	1.66, dt (3.2, 6.9)			
7	2.01, m	2.22, m	2.10, m	1.30, m
	1.54, dt (3.1, 12.0)			
8				1.58, m
				1.20, m
9	3.33, s	2.60, s	2.4, s	1.85, m
				1.30, m
11				2.11, m
12	1.46, s	1.47, s	1.36, s	0.95, d (6.9)
13	1.09, s	1.37, s	1.05, s	0.87, d (6.9)
14	1.05, s	1.09, s	0.96, s	1.05, s
15	1.33, s	1.14, s	1.25, s	1.50, s

[a] Measured in CD_3OD.
[b] Measured in $CDCl_3$.

2.4. Hydrolysis and methyl esterification reaction

A solution of **1** (15.0 mg) in THF (1.5 mL) was stirred with NaOH solution (1.0 M, 1.0 mL) at room temperature for 10 h. Then, the mixture was extracted with EtOAc, and the organic solution was evaporated under reduced pressure to yield the compound **8** (4.3 mg) and **9** (3.8 mg). While, the aqueous layer was acidified by HCl solution (1.0 M), and extracted with EtOAc. The organic solution was concentrated to give compound **14** (10.2 mg, Figs. S57–59). Trimethylsilyldiazomethane (1.0 mL) was added to a solution of **14** (9.6 mg) in MeOH (1.5 mL), and stirred at room temperature for 3 h. the mixture was extracted with EtOAc, and purified by Sephadex LH-20 CC (CH_2Cl_2/MeOH v/v, 1:1) to obtain **15** (7.6 mg, Fig. S60).

2.5. Preparation of the (S)- and (R) –MTPA esters *15a* and *15b*

Compound **15** (3.0 mg) was treated with (*R*)-MTPACl (15 μL) and pyridine (1.0 mL) at room temperature for 24 h. Then, the mixture was extracted with EtOAc, and the organic phase was concentrated. Finally, purification of the reaction mixture by preparative TLC yielded the (*S*)-MTPA ester **15a** (1.8 mg, Fig. S61). In a similar way, (*R*)-MTPA ester **15b** (1.8 mg, Fig. S61) was obtained.

(*S*)-MTPA ester **15a**: ^{1}H NMR ($CDCl_3$, 400 MHz) δ_H: 2.79 (H-2), 5.62 (H-3), 5.33 (H-4), 6.24 (H-5), 5.97 (H-6), 5.54 (H-7), 2.38 (H-8), 5.21 (H-9), 1.35 (H-10), 1.12 (H-11).

(*R*)-MTPA ester **15b**: ^{1}H NMR ($CDCl_3$, 400 MHz) δ_H: 2.77 (H-2), 5.65 (H-3), 5.47 (H-4), 6.38 (H-5), 6.08 (H-6), 5.71 (H-7), 2.45 (H-8), 5.21 (H-9), 1.30 (H-10), 1.08 (H-11).

2.6. Anti-inflammatory assay

The method for the assay of anti-inflammatory activity was according to the previously published paper [13]. N^G-monomethyl-$_L$-arginine ($_L$-NMMA) was used as positive control.

2.7. Molecular docking studies

The molecular docking study was accomplished in Sybyl-X 2.0, and

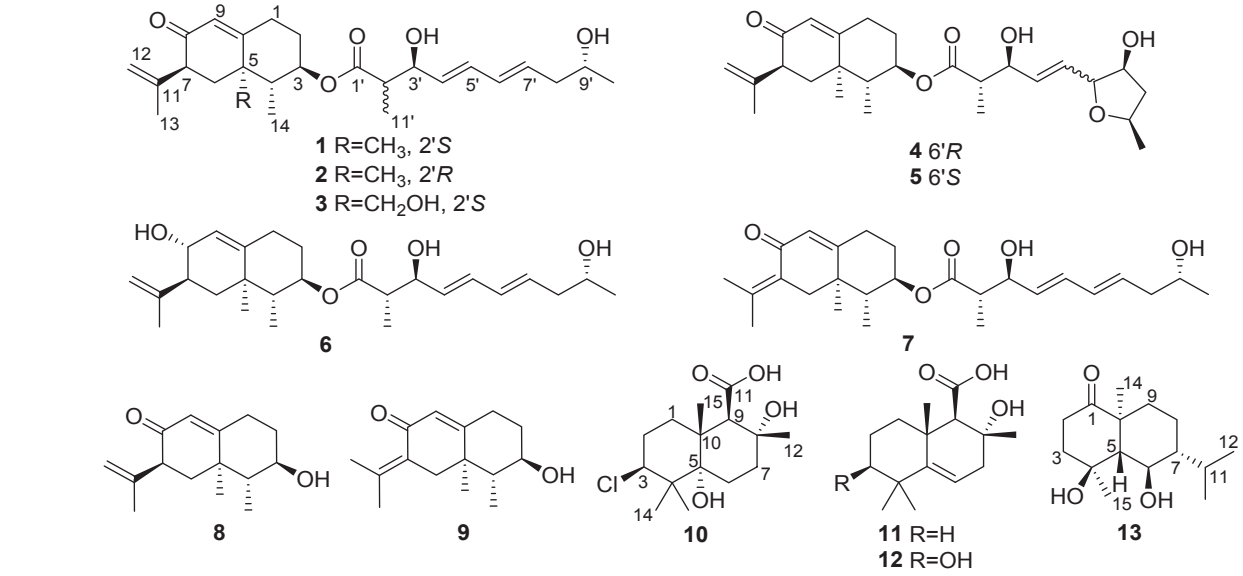

Fig. 1. Chemical structure of compounds **1**–**13**.

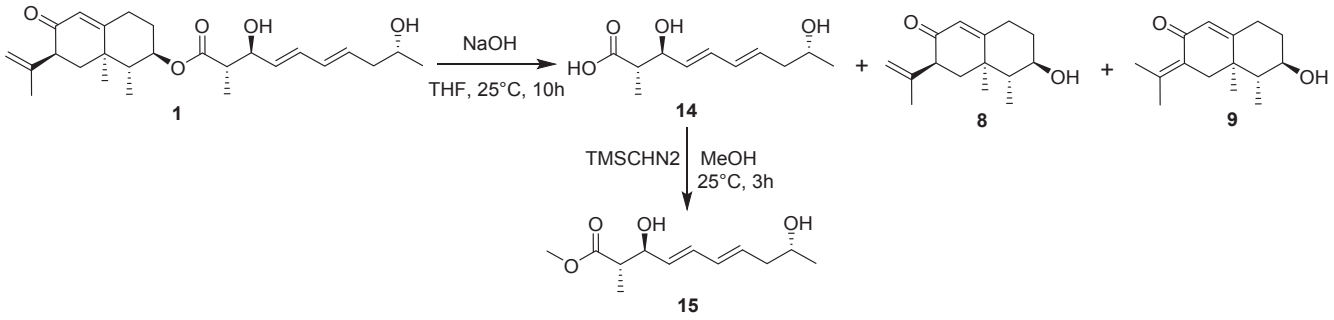

Scheme 1. Preparation of **15** from **1**.

crystal structure of iNOS (PDB: 3HR4) was obtained from the RCSB Protein Data Bank. The docking compounds **1**–**9** were first optimized with Gaussian 05 program at DFT calculations at B3LYP/6-21G (d) level. All polar hydrogen atoms were added and solvation parameters were assigned. Before the docking process, the ligand substructures were extracted and water molecules were removed. The surflex-dock total score was expressed in $-\mathrm{Log}(K_d)$ to represent binding affinities. The higher docking total score, the stronger interaction of proteins and bioactive compounds.

3. Result and discussion

Compounds **1**–**7** are eremophilane derivatives (Fig. 1), containing an eremophilane-type sesquiterpene moiety and a 3, 9-dihydroxy-2-methyldeca-4, 6-dienoic acid side chain. For the new eremophilane sesquiterpene derivatives **2** and **4**–**6**, their absolute configurations were determined based on that of the major component **1** (AA03390, Figs. S62–63 and Table S1) [14]. To establish the absolute configuration of **1**, it was hydrolyzed to give **14**, petasol (**8**) (Fig. S68–69) [15] and isopetasan (**9**) (Fig. S70–71) [16] (Scheme 1).

The configuration of the sesquiterpene moiety of **1** was assigned as 3*R*, 4*R*, 5*R*, 7*S* by the similar experimental ECD curves with (Fig. 5) and specific rotation of the hydrolyzed **8** obtained from **1** with those of **8** ($[\alpha]_D^{25}$ + 62, *c* 0.36, MeOH). For the side chain **14**, the double bonds were determined as 4′*E* and 6′*E* by the large coupling constants of $J_{\text{H-4′/H-5′}}$ = 15.1 Hz and $J_{\text{H-6′/H-7′}}$ = 15.0 Hz. The absolute configurations of the secondary alcohol at C-3′ and C-9′ were established by Mosher's method [13]. Compound **14** reaction with trimethylsilyldiazomethane in MeOH for three hours at the room temperature to yield **15**. Subsequently, the (*S*)-and (*R*)-MTPA esters of **15a** and **15b** were prepared using (*R*)-and (*S*)-MTPA chloride, respectively. The chemical shifts differences in ^{1}H NMR spectra (Fig. 2) were summarized and the absolute configuration at C-2′ and C-9′ were assigned as 2′*S,* 9′*R*. Moreover, the large coupling constant $^3J_{\text{H-2′, H-3′}}$ = 7.1 Hz indicated the *anti*-configuration [17] between CH_3-2′ and OH-3′. Thus, the absolute configuration of **1** was first determined as 3*R*, 4*R*, 5*R*, 7*S*, 2′*S*, 3′*S*, 9′*R*.

Compound **2** was isolated as a colorless oil. Its molecular formula of $C_{26}H_{38}O_5$ from HRESIMS was the same as compound **1**. The ^{1}H NMR data (Table 1) showed five methyl signals at δ_H 1.74 (s), 1.20 (s), 1.22 (d, *J* = 7.2 Hz), 1.23 (d, *J* = 6.1 Hz) and 0.96 (d, *J* = 6.6 Hz). Seven olefinic protons at δ_H 5.78 (brs), 5.01 (brs), 4.83 (brs), 5.62 (dd, *J* = 6.1, 15.2 Hz), 6.28 (dd, *J* = 10.3, 15.2 Hz), 6.12 (dd, *J* = 10.3, 15.0 Hz) and 5.73 (dt, *J* = 7.4, 15.0 Hz). The ^{13}C NMR data (Table 2) and HSQC spectra exhibited 26 carbon signals, containing five methyls, five methylenes

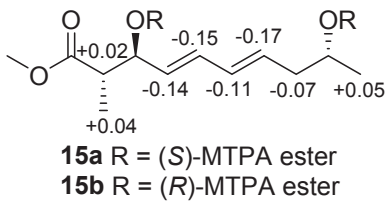

Fig. 2. $\Delta\delta = \delta_S - \delta_R$ values in ppm for the MTPA esters of **15**.

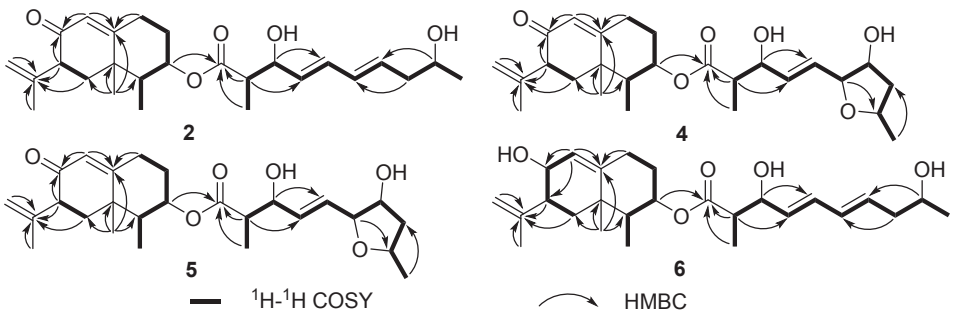

Fig. 3. Key HMBC and COSY correlations of compounds **2** and **4–6**.

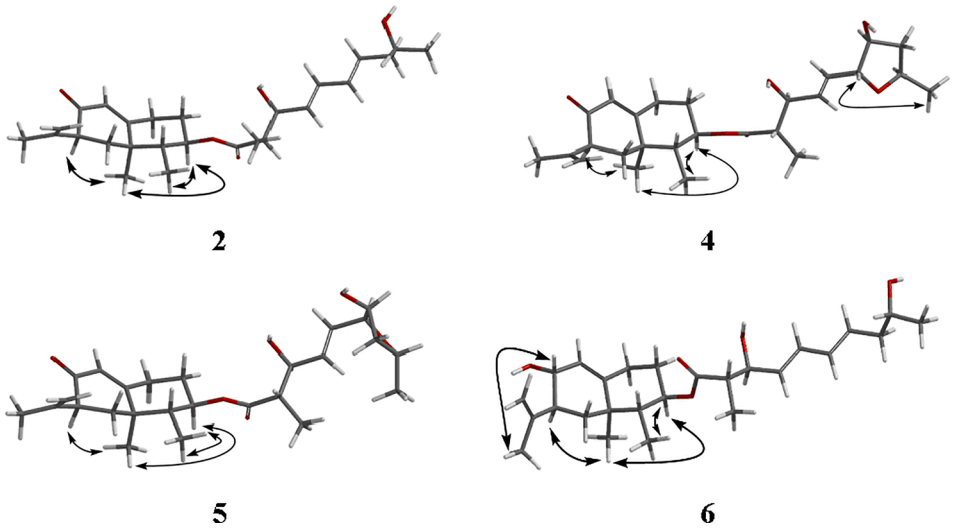

Fig. 4. Key NOESY correlations of compounds **2** and **4–6**.

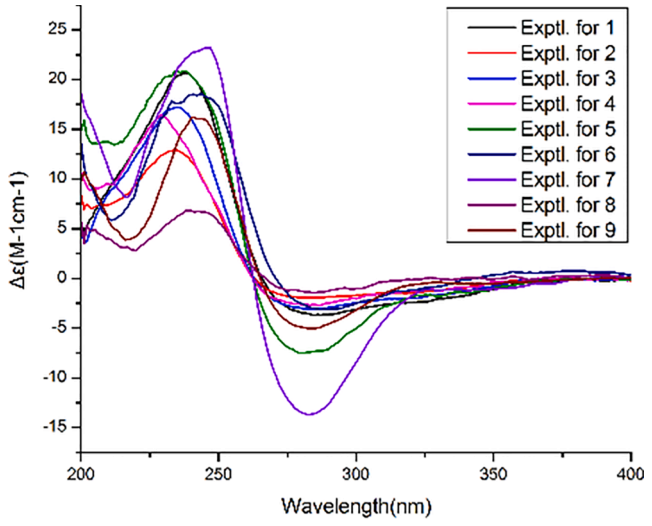

Fig. 5. Experimental ECD spectra of compounds **1**–**9** in methanol.

(one olefinic carbon), eleven methines (five olefinic carbons), five nonprotonated carbons (two carbonyl carbons and one olefinic carbon). The above data indicated that **2** was an eremophiane-type sesquiterpenoid. The ^{1}H-^{1}H COSY and HMBC correlations (Fig. 3) confirmed that compound **2** has the same planar structure as **1**. The same NOESY correlations (Fig. 4) of **1** and **2** revealed the relative configurations of the sesquiterpenoid moiety were similar. While, the difference of NMR shift at C-11′ in **1** (δ_C 14.1) and **2** (δ_C 11.6), implied the *erythro*-configuration between C2′-CH_3 and C3′-OH in **2** according to the Atsushi's report [18]. Furthermore, with the identical experimental ECD curves (Fig. 5), the absolute configurations of **2** were tentatively assigned as 3*R*, 4*R*, 5*R*, 7*S*, 2′*R*, 3′*S*, 9′*R* based on the shared biogenesis, and compound **2** was an epimer of compound **1** at C-2′.

The molecular formula of **4** and **5** were deduced via HRSEIMS as $C_{26}H_{38}O_6$, indicating 8 degrees of unsaturation. Their NMR data were similar to those of **1**, the major differences were that the olefinic carbons C-6′ (δ_C 132.4) and C-7′ (δ_C 131.3) in **1** were oxidized into the oxymethine C-6′ (δ_C 84.8) and C-7′ (δ_C 77.0) in **4**, as well as the oxymethine C-6′ (δ_C 86.5) and C-7′ (δ_C 77.4) in **5**. The above features were supported by the ^{1}H-^{1}H COSY cross-peak (Fig. 3) of H_3-11′/H-2′/H-3′/H-4′/H-5′/H-6′/H-7′/H_2-8′/H-9′/H_3-10′. The HMBC correlation from H-6′ to C-9′ indicated the presence of a tetrahydrofuran moiety in compounds **4** and **5**. The similar NOESY correlations (Fig. 4) and experimental ECD curves (Fig. 5) suggested that the absolute configuration in the eremophilane moiety were identical to those of **1**. The NOESY correlation of H-6′/H_3-10′ in the tetrahydrofuran ring was only observed in compound **4**, confirming that **4** was an epimer of **5** at C-6′. The coupling constant $^3J_{H\text{-}6'/H\text{-}7'}$ = 11.3 Hz in **4** and $^3J_{H\text{-}6'/H\text{-}7'}$ = 2.8 Hz in **5**, indicated that the relative configurations were determined as 6′*R*, 7′*S*, 9′*R* in **4** and 6′*S*, 7′*S*, 9′*R* in **5** [19,20]. Considering the biogenetic origin and the chemical shift at C-11′ (δ_C 14.1) in **4** and **5**, the stereochemistry at C-2′, C-3′ and C-9′ was assigned to be 2′*S*, 3′*S* and 9′*R*, respectively. Thus, the absolute configurations of **4** and **5** were tentatively assigned as 3*R*, 4*R*, 5*R*, 7*S*, 2′*S*, 3′*S*, 6′*R*, 7′*S*, 9′*R* and 3*R*, 4*R*, 5*R*, 7*S*, 2′S, 3′*S*, 6′*S*, 7′*S*, 9′*R*, respectively.

Compound **6** was isolated as a colorless oil and its molecular formula

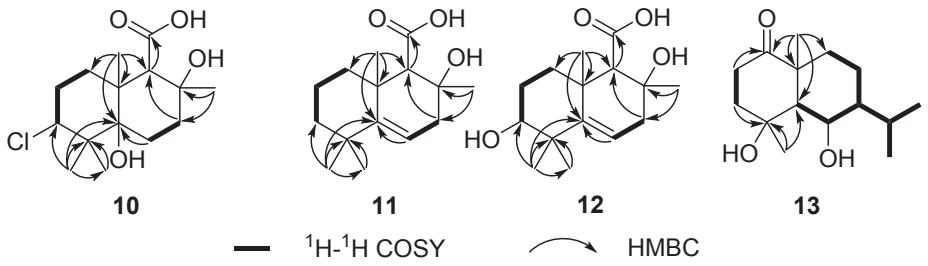

Fig. 6. Key HMBC and COSY correlations of compounds **10**–**13**.

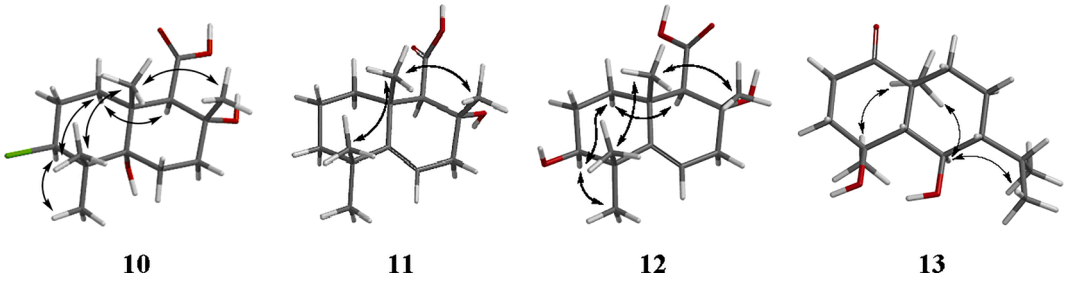

Fig. 7. Key NOESY correlations of compounds **10**–**13**.

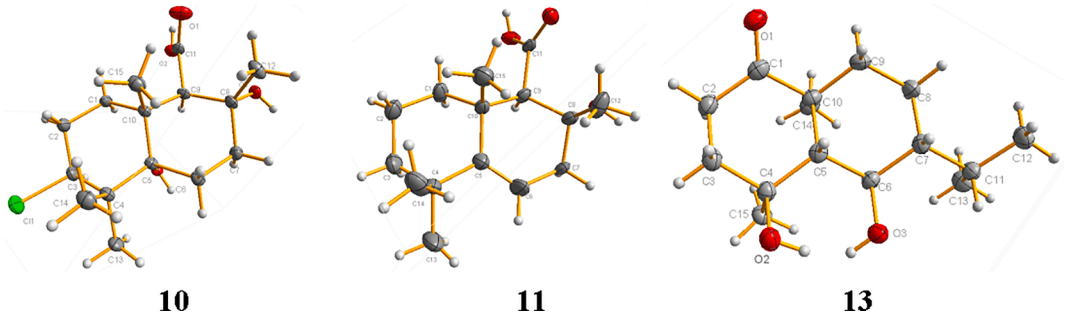

Fig. 8. X-ray crystallographic analysis of compounds **10**, **11** and **13**.

was deduced as $C_{26}H_{40}O_5$ based on HRESIMS data (*m/z* 455.27709 [M + Na]$^+$). The ^{1}H and ^{13}C NMR data (Tables 1 and 2) of compounds **1** and **6** displayed similar protons and carbon resonances, and revealed compound **6** to be an analogue of compound **1**. The main difference was the signals for the hydroxymethine group at C-8 (δ_H 4.09, brs and δ_C 63.6) in **6** replacing the ketone carbonyl carbon resonance (δ_C 198.6) in **1**, which was confirmed by the HMBC correlations from H-9 to C-8 and C-7, as well as the ^{1}H-^{1}H COSY cross-peaks of H-7/H-8/H-9. Finally, the structure of **6** was established. The relative configuration of the sesquiterpenoid moiety was assigned by NOESY data (Fig. 4) analysis. The cross peaks of H-3/H_3-14, H-3/H_3-15, H-7/H_3-15, H-8/H_3-13, confirmed that H-3, H_3-14, H_3-15 and H-7 were α-oriented, and H-8 was β-oriented. The limited quality of **6** making the Mosher's method was failed. Finally, the identical the experimental ECD curves of **1** and **6** (Fig. 5), indicated the 3*R*, 4*R*, 5*R*, 7*S*, 8*R* configuration of the sesquiterpene moiety. With the consideration of biogenetic origin, the configurations were tentatively assigned as 3*R*, 4*R*, 5*R*, 7*S*, 8*R*, 2′*S*, 3′*S*, 9′*R*.

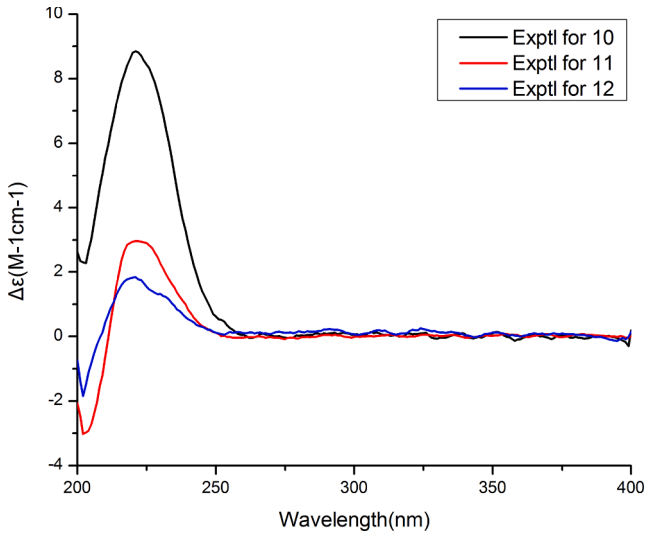

Fig. 9. Experimental ECD spectra of compounds **10**–**12** in methanol.

Compound **10** was isolated as colorless crystals. Its molecular

Table 4
Inhibitory activities of **1**–**13** against LPS-induced NO production.

Compound	IC_{50} (μM)	Compound	IC_{50} (μM)
1	14.5	**8**	22.5
2	13.5	**9**	18.0
3	12.0	**10**	45.0
4	8.6	**11**	50.0
5	9.2	**12**	42.5
6	13.5	**13**	50.0
7	10.5	$_L$-NMMA	15.0

formula was determined as $C_{15}H_{25}O_4Cl$ based on the HRESIMS spectrum. The ^1H NMR (Table 3) data showed four methyl signals at δ_H 1.46 (s), 1.33 (s), 1.09 (s) and 1.05 (s). The ^{13}C NMR (Table 2) and HSQC data exhibited 15 carbon signals, including four methyls, four methylenes, two methines, and five nonprotonated carbons (including one carbonyl). These NMR characteristics suggested that **10** was similar to diaporol I [21]. The downfield shift of C-5 (δ_C 78.5) revealed a hydroxyl group was linked to the C-5. Meanwhile, the HMBC correlation (Fig. 6) from H_3-13 to C-3, as well as the ^1H-^1H COSY cross-peaks of H_2-1/H_2-2/H-3, implied the chlorine atom was located at C-3. Therefore, the structure of **10** was established. The NOESY correlations (Fig. 7) of H-9/Ha-1/H-3/H_3-13, H_3-12/H_3-15/H_3-14, which suggested that H-3 and H-9 were α-oriented, and that H_3-12 and H_3-15 were β-oriented. Finally, the single-crystal X-ray crystallographic data of **10** [Flack parameter = 0.03 (3)] (Fig. 8) confirmed the structure and determined the absolute configuration as 3*S*, 5*S*, 8*R*, 9*R*, 10*R*.

Compound **11** was isolated as colorless crystals with the molecular formula $C_{15}H_{24}O_3$. A comparison of the 1D NMR data of **11** with those of **10** revealed the similar structure of two compounds. The structure of **11** was established by extensive analysis of ^1H-^1H COSY and HMBC correlations (Fig. 6). While, the planar structure was identified the same as a synthetic intermediate [22] using SciFinder (CAS Registry Number: 501649-02-1). Then, the single-crystal X-ray crystallography results [Flack parameter = −0.04 (16)] (Fig. 8) confirmed the structure including the 8*R*, 9*R*, 10*R* absolute configuration.

Compound **12** was obtained as a white solid with the molecular

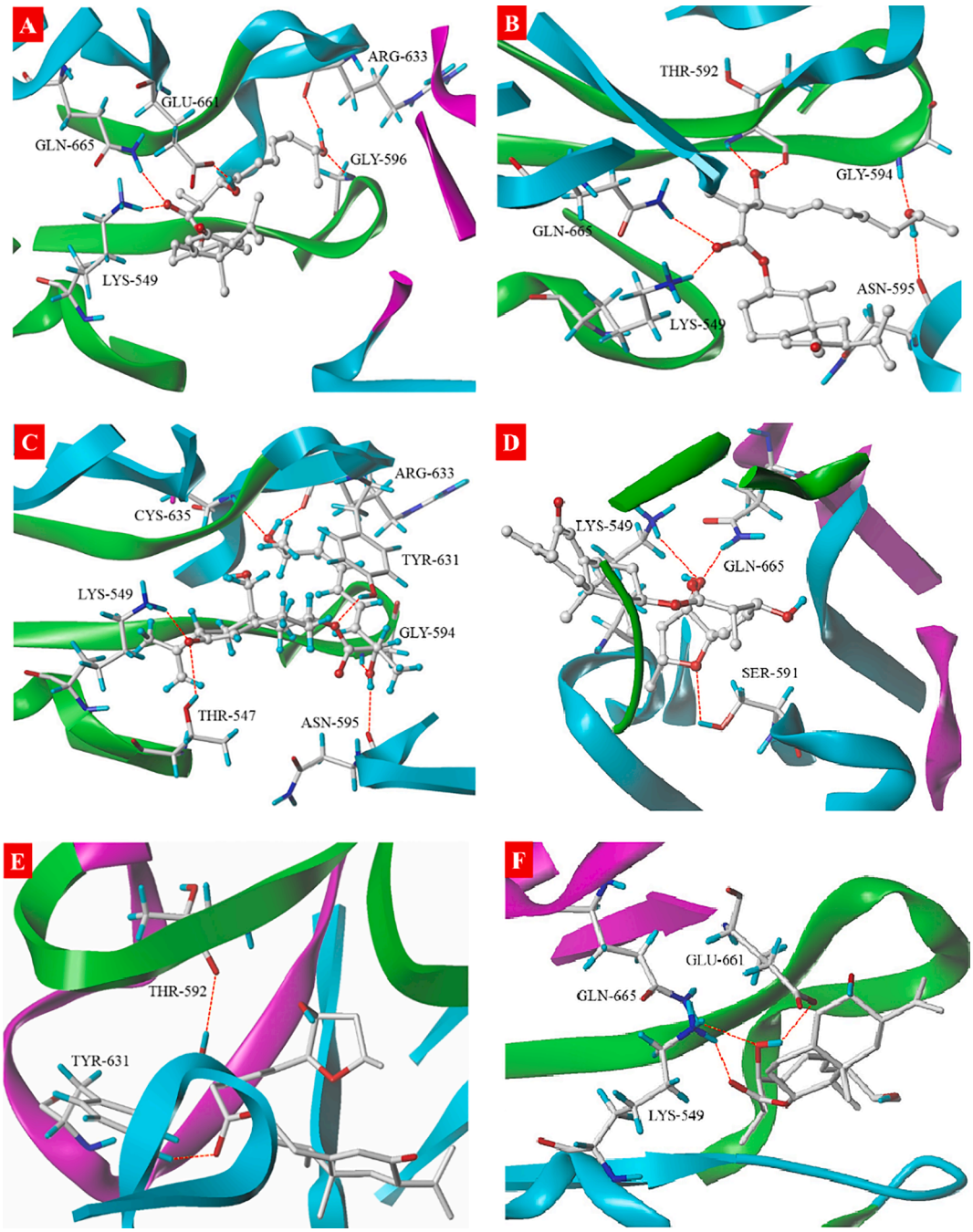

Fig. 10. Molecular docking simulations obtained at the lowest energy conformation, highlighting potential hydrogen contacts of compounds **1** (A), **2** (B), **3** (C), **4** (D), **5** (E), **6** (F), **7** (G), **8** (H), **9** (I), respectively. Only interacting residues are labeled, and hydrogen bonding interactions are shown by red dashes. (For interpretation of the references to colour in this figure legend, the reader is referred to the web version of this article.)

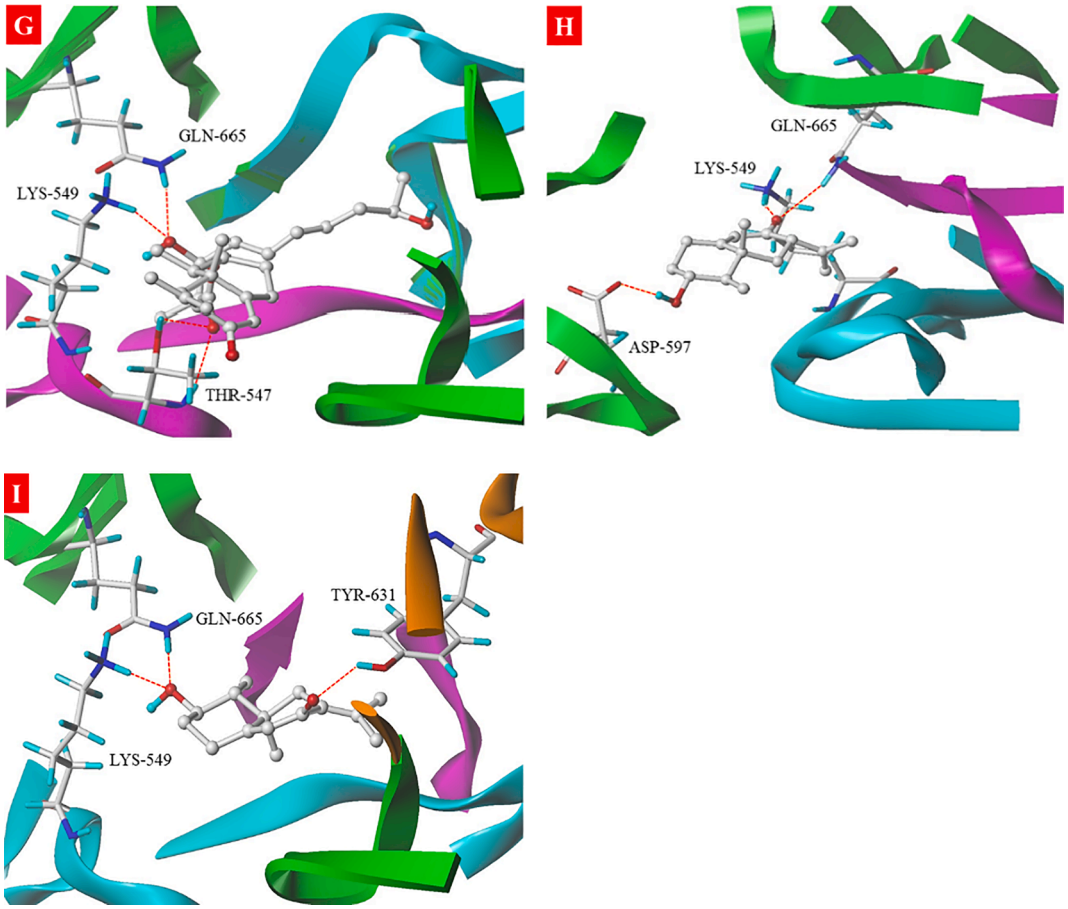

Fig. 10. (*continued*).

formula of $C_{15}H_{24}O_4$ by HRESIMS spectrum. The ^1H and ^{13}C NMR data (Table 2 and 3) were similar to those of **11**, revealing that **12** shared the same skeleton with **11**. The HMBC correlations from H_3-14 to C-3 and the ^1H-^1H COSY cross-peaks of H_2-1/H_2-2/H-3 (Fig. 6), suggested that compound **12** was the 3-hydroxy derivative of **11**. The NOESY correlations (Fig. 7) of H-9/Ha-1/H-3/H_3-13, H_3-12/H_3-15/H_3-14, confirmed that H-3 and H-9 were α-oriented. Furthermore, the absolute configuration of **11** was established as 3*S*, 8*R*, 9*R*, 10*R* by the identical experimental ECD curves to **10** and **11** (Fig. 9).

Compound **13** was obtained as colorless crystals and yield molecular formula $C_{15}H_{26}O_3$. The ^1H NMR spectra showed four methyl signals at δ_H 1.50 (s), 1.05 (s), 0.95 (d, $J = 6.9$ Hz) and 0.87 (d, $J = 6.9$ Hz) and one oxygenated methine proton δ_H 3.88 (t, $J = 10.2$ Hz). The ^{13}C NMR data (Table 2) exhibited 15 carbon signals, including four methyls, four methylenes, four methines and three nonprotonated carbons (including one carbonyl). These data indicated that **13** was a bicyclic sesquiterpene [23]. The planar structure of **13** was confirmed by the 2D NMR data. The spin systems of H_2-2/H_2-3, and H-5/H-6/H-7($/H_2$-8/H_2-9)/H-11($/H_3$-12)/H_3-13, together with the HMBC correlations (Fig. 6) from H_2-2 to C-1, from H_2-3 to C-4, from H_3-14 to C-1, C-9 and C-10 and from H_3-15 to C-4 and C-5, established the compound **13** was a eudesmane-type sesquiterpene derivative. The NOESY correlations (Fig. 7) of H_3-12/H-6($/H_3$-15)/H_3-14, indicated the H-6, H_3-12, H_3-14, H_3-15 protons were α-oriented. The large coupling constant of $^3J_{H\text{-}5/H\text{-}6} = 10.2$ Hz revealed the β-oriented of H-5. Subsequently, the single-crystal X-ray diffraction analysis determined the absolute configuration of **13** (Fig. 8) as 4*S*, 5*R*, 6*R*, 7*R*, 10*S*.

Compounds **3** and **7** were identified as eremofortin F (Fig. S64–65) [14] and lithocarin A (Fig. S66–67) [24], respectively, by comparison of the spectroscopic data (Table S1) with the literature. Until now, their absolute configurations of the side chain at C-3 were not determined. The similar experiment ECD curves (Fig. 5) indicated that the configuration in the eremophilane moiety of **3** and **7** were the same as those of **1**. With the consideration of biogenetic origin, and the comparison of NMR shift at C-11′ (**1:** δ_C 14.1; **3**: δ_C 14.2; **7**: δ_C 14.2), the stereochemistry of side chain in **1**, **3** and **7** were identical. Taken together, the absolute configurations of **3** and **7** were tentatively assigned as 3*R*, 4*R*, 5*R*, 7*S*, 2′*S*, 3′*S*, 9′*R* and 3*R*, 4*R*, 5*R*, 2′*S*, 3′*S*, 9′*R*, respectively.

The other known compounds were identified as petasol (**8**) [15] and isopetasan (**9**) [15], by comparison the spectroscopic data with the literature.

On considering the significant inhibitory activities against nitric oxide (NO) production in lipopolysaccharides (LPS) induced RAW 264.7 cells of the crude extract, the NO inhibitory activity of the obtained sesquiterpene derivatives (**1**–**13**) were evaluated (Table 4). Compounds **4** and **5** showed potent inhibitory activities with IC_{50} values of 8.6 and 9.2 μM, respectively. Compounds **1**–**3** and **6**–**9** exhibited moderate inhibitory activities with IC_{50} values ranging from 10.5 to 22.5 μM. The positive control was used N^G-monomethyl-$_L$-arginine ($_L$-NMMA) with IC_{50} value of 15.0 μM. All compounds showed no cytotoxic effect at the tested concentration.

The inducible NOS (iNOS), which was the one types of NOS, was critical to the NO production in the inflammation occurs [25]. To investigate the underlying mechanism of bioactive compounds and nitric oxide synthase, a molecular docking study was performed. Molecular Docking is a theoretical simulation method that simulate the interaction of ligand-protein, and predict the binding patterns and affinity [26–27]. Compounds **1**–**9**, which have the most potent inhibitory effects ($IC_{50} < 22.5$ μM), were selected for the molecular docking. As shown in Fig. 10, the most active NO inhibitor **4** showed three hydrogen

Table 5
Logarithms of free binding energies (FBE, kcal/mol) of NO inhibitors to the avtive cavities of iNOS (PDB code: 3HR4) and targeting rsidues of the binding site located on the mobile flap.

Compound	−Log (FBE)	Targeting residues
1	− 2.9	GLN-665, GLU-661, LYS-549, ARG-633, GLY-596
2	−8.2	GLN-665, THR-592, GLY-549, LYS-549, ASN-595
3	−10.9	CSY-635, ARG-633, TYR-631, GLY-594, LYS-549, THR-547 ASN-595
4	−8.3	LYS-549, GLN-665, SER-591
5	−8.0	THR-592, TYR-631
6	−6.9	GLU-661, GLN-665, LYS-549
7	−7.5	GLN-665, LYS-549, THR-547
8	−6.6	GLN-665, LYS-549, ASP-597
9	−7.3	GLN-665, LYS-549, TYR-631

bonds with the residues of LYS-549, GLN-665 and SER-591. Similarly, two hydrogen bonds were formed in compound **5**, including the hydroxyl group at C-3′ with THR-592 and the carbonyl group with TYR-631. The binding energy of compounds **4** and **5** with the active cavity of iNOS were −8.3 and −8.0 kcal/mol, respectively. Then, the binding residues and the logarithm of free binding energy were collated in Table 5. The docking results provided an inside interaction of **1**–**9** with iNOS and revealed the possible mechanism of NO inhibition of bioactive compounds binding with the residues of the active cavities.

4. Conclusion

In summary, eight new sesquiterpene derivatives (**2**, **4**–**6** and **10**–**13**) and five known analogues (**1**, **3** and **7**–**9**) were isolated from the mangrove endophytic fungus *Phomopsis* sp. SYSU-QYP-23. For the absolute configuration of eremophilane sesquiterpenes, the side chain of **1** was the first defined by modified Mosher's method. Compounds **4** and **5** showed the potent NO inhibitory activity with the IC_{50} values of 8.6 and 9.2 μM, respectively. Compounds **1**–**3** and **6**–**7** exhibited moderate inhibitory activity compared to the positive control ($_L$-NMMA: 15.0 μM). Moreover, a better activity of compounds **1**–**7** than **8**–**9**, showed that the said chain at C-3 make a contribution to the NO inhibitory activity. Finally, the binding interaction of bioactive compounds **1**–**9** with iNOS protein were researched by molecular docking studies. The eremophilane-type sesquiterpenes were reported to have anti-inflammatory activity [28–31]. This study suggested that the eremophilane-type sesquiterpenes could further researched as the anti-inflammatory therapeutic lead compounds.

Declaration of Competing Interest

The authors declare that they have no known competing financial interests or personal relationships that could have appeared to influence the work reported in this paper.

Acknowledgements

We thank the National Key R&D Program of China (2019YFC0312501), the National Natural Science Foundation of China (21877133, 41876153 and 41906033), the Key Project of Natural Science Foundation of Guangdong Province (2016A030311026), the Natural Science Foundation of Guangdong Province of China (grant number 2019A1515012084), and PHD researchers of Guangdong Medical University (grant number B2017028) for generous support.

Appendix A. Supplementary material

The 1D and 2D NMR, HRESIMS spectra of compounds **2**, **4**–**6**, **10**–**13**, the ^{1}H and ^{13}C NMR spectra of the known compounds **1**, **3** and **7**-**9**, the 1D NMR data of known compounds **1**, **3**, **7** and the X-ray data for **10**, **11** and **13** (CIF) are available free of charge via the internet.

Supplementary data to this article can be found online at https://doi.org/10.1016/j.bioorg.2020.104530.

References

[1] N. Duhamel, D. Slaghenaufi, L.I. Pilkington, M.H. Johnstone, R. Larcher, D. Barker, B. Fedrizzi, J. Chromatogr. A. 1537 (2018) 91–98.
[2] A. Modzelewska, S. Sur, S.K. Kumar, S.R. Khan, Curr. Med. Chem. Anti-Cancer Agents 5 (2005) 477–499.
[3] L.F. Bideau, M. Kousara, L. Chen, L. Wei, F. Dumas, Chem. Rev. 117 (2017) 6110–6159.
[4] J. Liu, D. Zhang, M. Zhang, J.L. Zhao, R.D. Chen, N. Wang, D. Zhang, J.G. Dai, J. Nat. Prod. 79 (2016) 2229–2235.
[5] S. Stefania, M. Filippo, N. Marcello, B. Valeria, D. Stefano, Curr. Med. Chem. 25 (2018) 1241–1258.
[6] M.J. Durán-Peña, J.M.B. Ares, J.R. Hanson, I.G. Collado, Nat. Prod. Rep. 32 (2015) 1236–1248.
[7] A.C. Spivey, M. Weston, S. Woodhead, Chem. Soc. Rev. 31 (2002) 43–59.
[8] Z.X. Hu, Y. Wu, S.S. Xie, W.G. Sun, Y. Guo, X.N. Li, J.J. Liu, Y.B. Xue, Y.H. Zhang, Org. lett. 19 (2016), 258–26.
[9] S.S. Xie, Y. Wu, Y.B. Qiao, Y. Guo, J.P. Wang, Z.X. Hu, Q. Zhang, Y.B. Xue, Y. H. Zhang, J. Nat. Prod. 81 (2018) 1311–1320.
[10] C. Hemtasin, S. Kanokmedhakul, K. Kanokmedhakul, C. Hahnvajanawong, K. Soytong, S. Prabpai, P. Kongsaeree, J. Nat. Prod. 74 (2011) 609–613.
[11] J.L. Xu, Z.M. Liu, Y.C. Chen, H.B. Tian, H.H. Li, S.N. Li, H. Guo, Z.L. Huang, X. X. Gao, H.X. Liu, W.M. Zhang, Bioorg. Chem. 87 (2019) 728–735.
[12] Y. Chen, L.S. Zhang, G. Zou, W.C. Yang, H.J. Liu, Z.G. She, Bioorg. Chem. 97 (2020), 103712.
[13] Y. Chen, Z.M. Liu, H.J. Liu, Y.H. Pan, J. Li, L. Liu, Z.G. She, Mar. Drugs 16 (2018) 54.
[14] H. Mandavid, A.M.S. Rodrigues, L.S. Espindola, V. Eparvier, D. Stien, J. Nat. Prod. 78 (2015) 1735–1739.
[15] D.H. Le, Y. Takenaka, N. Hamada, T. Tanahashi, Phytochemistry 91 (2013) 242–248.
[16] C. Daengrot, V. Rukachaisirikul, C. Tansakul, T. Thongpanchang, S. Phongpaichit, K. Bowornwiriyapan, J. Sskayaroj, J. Nat. Prod. 78 (2015) 615–622.
[17] G.E. Chlipala, P.H. Tri, N.V. Hung, A. Krunic, S.H. Shim, D.D. Soejarto, J. Orjala, J. Nat. Prod. 73 (2010) 784–787.
[18] A. Ito, I. Kumagai, M. Maruyama, H. Maeda, A. Tonouchi, T. Nehira, K.I. Kimura, M. Hashimoto, Tetrahedron Lett. 57 (2016) 1117–1119.
[19] Y.C. Shen, C.Y. Chen, Y.M. Lin, Y.H. Kuo, Phytochemistry 46 (1997) 1111–1113.
[20] H.M.T. Bandara Herath, A.M. Anoma Priyadarshani, Phytochemistry 42 (1996) 1439–1442.
[21] L.Y. Zang, W. Wei, Y. Guo, T. Wang, R.H. Jiao, S.W. Ng, R.X. Tan, H.M. Ge, J. Nat. Prod. 75 (2012) 1744–1749.
[22] S. Yasuaki, K. Yukihiro, I. Akitami, S. Sadao, Tomakomai Kogyo Koto Senmon Gakko Kiyo 37 (2002) 115–119.
[23] W.M. Zhu, Q. Zhao, S.L. Li, X.J. Hao, J. Asian Nat. Prod. Res. 9 (2007) 277–283.
[24] J.L. Xu, H.X. Liu, Y.C. Chen, H.B. Tan, H. Guo, L.Q. Xu, S.N. Li, Z.L. Huang, H.H. Li, X.X. Gao, W.M. Zhang, Mar. Drugs 16 (2018) 329.
[25] A.H. Wang, A.Z. Song, A.H. Xing, Z.Y. Shi, P. Wu, J. Zhang, M. Tuerhong, J. Xu, Y. Q. Guo, Bioorg. Chem. 101 (2020), 103974.
[26] J. Xu, M.C. Wang, X.C. Sun, Q.H. Ren, X.R. Cao, S. Li, G.C. Su, M. Tuerhong, D. Lee, Y. Ohizumi, M. Bartlam, Y.Q. Guo, J. Nat. Prod. 79 (2016) 2924–2932.
[27] D. Tang, Y.Z. Xu, W.W. Wang, Z. Yang, B. Liu, M. Stadler, L.L. Liu, J.M. Gao, J. Nat. Prod. 82 (2019) 1599–1608.
[28] J.C. Chang, G. Hsiao, R.K. Lin, R.K. Lin, Y.H. Kuo, Y.M. Ju, T.H. Lee, J. Nat. Prod. 80 (2017) 38–44.
[29] J.H. Zhao, T. Shen, X. Yang, H. Zhao, X. Li, W.D. Xie, Arch. Pharm. Res. 35 (2012) 1153–1158.
[30] A. Arciniegas, K. Gonzalez, A.L. Perez-Castorena, J. Maldonado, J.L. Villasenor, J. Nat. Prod. 74 (2011) 1584–1589.
[31] B.Y. Hwang, J. Lee, T.H. Koo, H.S. Kim, Y.S. Hong, J.S. Ro, K.S. Lee, J.J. Lee, Planta Med. 68 (2002) 101–105.